**RESEARCH PAPER**

# A low-resistance hybrid nanomaterial composed of double-charged ionic liquid and a layered double hydroxide (type Al/Mg-dodecyl sulfate) for electrochemical determination of methyldopa

*Mir Mahdi Abolghasemi\*, Marzieh Piryaei , Elnaz Tartibi*

*Department of Chemistry, Faculty of Science, University of Maragheh, Maragheh, Iran*

**ARTICLE INFO**

**ABSTRACT**

The quantification and electrochemical behavior of methyldopa in tablet and urine samples were carried out using a glassy carbon electrode modified with double-charged ionic liquid and a layered double hydroxide. Magnesium aluminum layered double hydroxides/double charged diazabicyclo [2.2.2] octane ionic liquid (Mg/Al LDH/DABCO-IL) was prepared and immobilized on a glassy carbon electrode. The results of Fourier transform infrared spectroscopy (FT-IR) and X-ray diffraction (XRD) demonstrated that Mg/Al LDH/DABCO-IL was successfully synthesized. The cyclic voltammogram of methyldopa on the modified electrode exhibited a well-defined anodic peak at 0.63 V in 0.1 M of ammonia buffer. The experimental parameters were optimized and the kinetic parameters were investigated. Under the optimized conditions, the fabricated modified electrode exhibited excellent performance in the linear range of 0.23-860 μM with a correlation coefficient of 0.9959. The detection limit was 0.076 μM (S/N = 3). The fabricated electrode showed good reproducibility, stability, and selectivity properties. The method was successfully applied for the determination of methyldopa in pharmaceutical and urine samples.

## INTRODUCTION

Methyldopa (m-dopa) (l-a-methyl-3, 4-dihydrophenylalanine) is an antihypertensive agent widely used in the treatment and control of hypertension or high blood pressure particularly during pregnancy. Methyldopa (Fig. S1) undergoes reduction to α-methyl norepinephrine in adrenergic nerve terminus and plays a major role in the central nervous system. It is a centrally acting $a_2$-adreno receptor agonist that reduces sympathetic tone and results in a decline in blood pressure. Methyldopa is capable of inducing a number of adverse side effects such as nervous system depressant effects including dizziness, tiredness, depression, bloating, constipation, diarrhea, dizziness, extreme drowsiness, light-headedness, nausea, severely low blood pressure, slow heartbeat, vomiting, and weakness. In addition, the long-term use or excessive intake of methyldopa may lead to hepatotoxicity and anemia [1]. Therefore, detection and determination of methyldopa in low concentration levels are necessary and researchers have considered this issue. Many techniques have been examined for the determination of m-dopa including chromatography techniques (HPLC, HPTLC, LC-MS, GC), photometric techniques (fluorescence, UV-visible, chemiluminescence, NMR spectroscopy), and electrochemical techniques [2-6]. Among these methods,

\* Corresponding Author Email: *mehdiabolghasemi@gmail.com*

electrochemical techniques have many advantages for pharmaceutical analysis including fast response, cheap instrument, low cost, simple operation, timesaving, high sensitivity, good selectivity, and possibility of miniaturization [7].

Methyldopa has a catecholamine structure, and hydroxyl groups within the molecule can oxide to carbonyl groups (quinone). This reaction happens at high overpotentials on bare electrodes and low current densities are obtained which increase the interference of determination, leading to low selectivity and sensitivity as well as low oxidation peak current. Therefore, m-dopa determination based on electrochemical method is usually performed on modified electrodes [8]. On the other hand, the electrocatalytic activities of modified electrodes strongly depend on their surface structures and electrochemical catalytic behaviors. In recent years, inorganic clays have been widely employed for the fabrication of sensors due to their high ion-exchange capacity, good adsorption property, special structural feature, high storage stability, and chemical stability.

An important type of ionic lamellar inorganic nanomaterials is considered as layered double hydroxides (LDH), which is called anionic clays. The structure of LDHs is characterized by positive charge brucite-like sheets, and anions intercalation in the hydrated interlayer regions balance these positive charges. The general formula of LDH is $[M(II)_{1-x} M(III)_x (OH)_2]^{x+} [A^{n-}]_{x/n} .mH_2O$ which M III denotes trivalent metal ions, M II represents divalent metal ions, A is the charge compensating anions, m is the number of moles of co-intercalated water per formula weight of compounds, and x is the number of moles of M III per formula weight of compounds.

LDHs are recognized as potential materials for ion exchangers, catalysts, pharmaceutics, adsorbents, catalyst supports and so on; these features of LDHs are attributed to their large surface areas, great anionic exchange capacity, catalytic activity, and adsorption property [9, 10].

Nevertheless, since LDHs are hydrophilic structure, inorganic parent LDH crystallites have low sorption affinity for organic compounds in water [11]. LDH surface properties can be altered from hydrophilic to hydrophobic by organic compounds intercalation into the interlayer which results in an increased sorption capacity for organic compounds [12].

In this study, we reported an interlayer surface modification of LDH with double-charged diazabicyclo [2.2.2] octane ionic liquid (IL) for continuing our previous studies on employing LDHs [13]. In this method, we prepared dodecyl sulfate intercalated LDH using co-precipitation approach. Organ silane containing bridged double-charged diazabicyclo[2.2.2]octane dichloride groups as a precursor was then added to the prepared LDH-DABCO-IL inorganic organic hybrid materials. Recently, the mentioned designed LDH-IL is found to have high extraction efficiency for the organic compounds in water samples. Therefore, employing LDH-DABCO-IL as a modified electrode coating was investigated. Integrating of ionic liquid and LDHs provides organic–inorganic hybrid nanomaterials which enable us to expand electrochemical methods. In this approach, the linear range, limit of detection reproducibility, and sensitivity of method were obtained at a trace level in aqueous matrices to evaluate the performance of the modified LDH-DABCO-IL electrode. The effective factors influencing the electrochemical oxidation of m-dopa were precisely studied. Furthermore, in order to specify trace amounts of m-dopa in urine samples and tablet, the proposed approach was employed.

# EXPERIMENTAL
## *Materials and instruments*
### Materials

Methyldopa was purchased from Darou pakhsh Co. (www.dppharma.com). 0.1 M of methyldopa stock solution was prepared with methanol and kept in refrigerator at 4 ºC. Working solutions were freshly prepared before use by diluting the stock solution. 0.1 M ammonia buffer was prepared and the pH with HCl or NaOH was adjusted. All other reagents were of analytical reagent grade and used as received without further purification. All chemicals employed in this work including DABCO, NaOH, KBr, KI, $Na_2SO_4$, $KClO_3$, $KIO_3$, HCl (37%), $H_3PO_4$ (85%), $K_3Fe(CN)_6$, $K_2HPO_4$, $KH_2PO_4$ and acetone were purchased from Merck (www.merckgroup.com). All the solutions were prepared with deionized water.

### Apparatus

The electrochemical studies were accomplished with a μ–Autolab III (potentiostat, galvanostat) instrument equipped with three electrodes, a USB port, and the GPES 4.9.007 software. Pt wire (Metrohm, Netherland) and Ag/AgCl (3 M KCl)

10

*Nanochem. Res., 9(1): 9-18, Winter 2024*

were used as the counter electrode and reference electrode, respectively. The glassy carbon electrode (GCE; 1.0 mm diameter, 0.0314 cm$^2$ area) served as the working electrode.

Fourier transform infrared (FT-IR) spectra were recorded on a Perkin-Elmer Spectrum GX spectrometer. Powder X-ray diffraction (XRD) patterns were recorded using a Rigaku D/MAX 2200PC X-ray diffractometer (Japan) with Cu Kα radiation (λ = 0.154178 nm, graphite monochromator, 28 Kv and 20 mA). A 2θ range from 5 to 75 was investigated at a scanning speed of 10º min⁻¹. Scanning electron microscopy (SEM) was performed on a Hitachi S-3000N instrument (Japan). The pH measurements were carried out with a Metrohm pH meter model 744 (Switzerland), which was calibrated with standard pH buffer. All the measurements were performed at room temperature.

**Synthesis of LDH-dodecyl sulfate and LDH-DABCO-IL**

The Al/Mg-dodecyl sulfate LDH and LDH-DABCO-IL were synthesized according to the previous report (see supporting information) [14].

**Preparation of LDH-DABCO-IL electrodes**

The glassy carbon electrode (GCE) was polished with alumina powder before starting each experiment and modification step. After polishing, to remove the remaining amounts of alumina from the electrode surface, the surface of electrode was washed with water and ultrasonicated in an ultrasonic water bath (in ethanol/water, 1:1 v: v). Subsequently, 5μL of the modifier (1 mg.mL⁻¹) was dropped on the GCE with a micro syringe and dried at room temperature. The schematic of preparation nanostructure LDH-DABCO-IL electrode is shown in Fig. S2.

**Preparation of real samples**

In order to prepare real samples of methyldopa tablets, initially, 10 tablets of methyldopa (purchased from Darou pakhsh Co.) were thoroughly ground in mortar. Then, 0.38 g of powder, equivalent to the weight of one tablet, was dissolved in 10 mL methanol by ultrasonication for 30 min. Finally, the solution was filtered, and the filtrate was diluted to 50 mL using 0.1 M ammonia buffer. Urine samples were diluted 5 times with ammonia buffer before recording differential pulse voltammetry.

**RESULT AND DISCUSSION**

*Electrochemical behaviors of LDH-DABCO-IL modified glassy carbon electrode*

The electrochemical properties of a bare GCE and modified electrodes were characterized by cyclic voltammetry (CV) and electrochemical impedance spectroscopy (EIS). Fig. 1A depicts CVs of the bare GCE, layered double hydroxides-nitrate modified GCE (LDH-NO$_3$/GCE), the magnesium aluminum layered double hydroxides-dodecyl sulfate modified GCE (Mg/Al-SDS/LDH/ GCE), and LDH-DABCO-IL/GCE in 5 mM K$_3$ [Fe (CN)$_6$] and 1 M KCl (1:1 v: v) as a redox probe. As can be seen, a few redox peaks with peak-to-peak separation (ΔEp) of 0.5 V, which is appropriately defined, is demonstrated by the bare GCE. A drop in peak currents (Ip) and an increase in Ep were noticed once the electrode was coated with LDH. As it is recognized, [Fe(CN)$_6$]$^{3-/4-}$ anions can incorporate into LDH coating which is possible by long range electrostatic interactions with positive LDH charge surface. It may result in the reduction of the electron transfer rate which is caused by switching from an aqueous phase to an LDH one [15]. In other words, the electron transfer rate between electrode surface and Fe(CN)$_6$$^{3-/4-}$ is reduced by the LDH immobilization.

In addition, LDH-SDS/GCE shows less peak current than the bare GCE and LDH/GCE. The literature reports that the thickness of Mg AL-LDH is 0.48-nm and that of Mg AL-SDS-LDH is 2.27 nm. This suggests that the tails of SDS anions are intercalated in the inter lamellar space of LDH. The intercalation of SDS anions in LDH layers increases the lipophilicity of the structure. As a result affinity of the of [Fe(CN)$_6$]$^{3-/4-}$ into the LDH layer extremely decreasing. thus, an increase in Ep and a decrease in peak currents (Ip) were observed.

As can be seen in Fig. 1A, the ΔEp (0.22 V) at the LDH-DABCO-IL/GCE is significantly smaller than that at the LDH-NO$_3$/GCE (0.72 V), bare GC (0.51 V) and LDH-SDS/GCE (1.1 V) electrodes. It is also indicated that there has been an improvement in the reversibility of electrochemical reaction, and simultaneously a significant increase in the redox peak currents. The strong adsorptive abilities and higher surface area of LDH-DABCO-IL/GCE film may account for this observation. As a result, [Fe(CN)6]$^{3-/4-}$ exhibits a highly effective accumulation efficiency and an improved surface concentration.
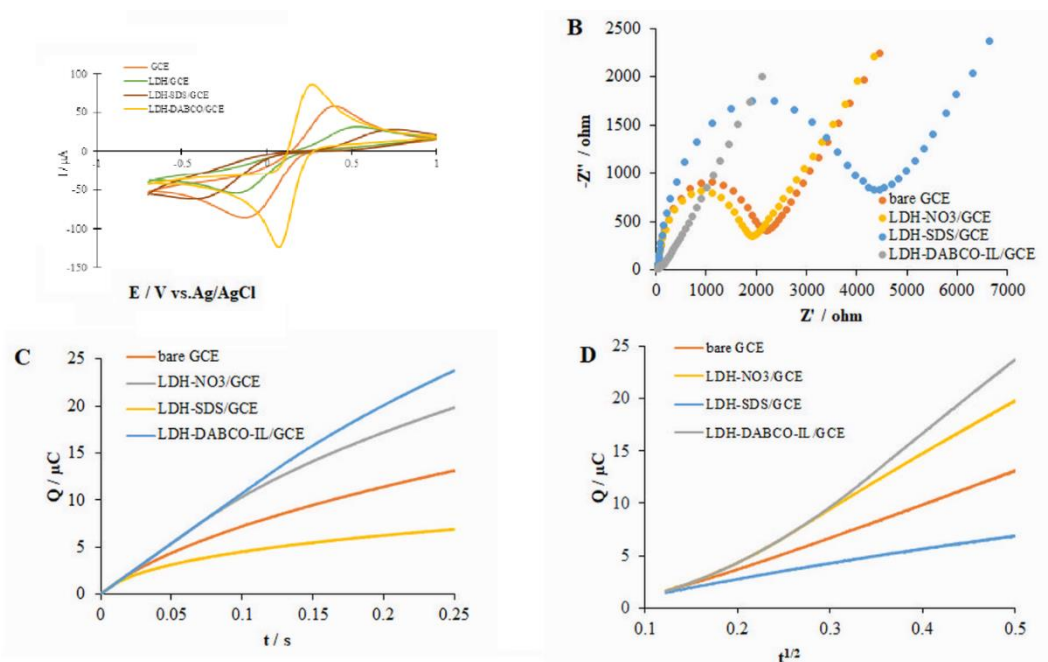
The high polarity of the double charge DABCO-

*Nanochem. Res., 9(1): 9-18, Winter 2024*

11

Fig. 1. Cyclic voltammograms (A) and Nyquist plots (B) of bare GCE, LDH-NO₃/GCE, LDH-SDS/GCE and LDH-DABCO-IL in 2.5 mM Fe(CN)$_6^{3-/4-}$ (1:1) solution containing 0.5 M KCl. Scan rate: 50 mV.s$^{-1}$. The frequency range was from 0.1 to 10⁵ Hz at the formal potential of 0.18 V. Plot of Q–t curve (C) and plot of Q–t$^{1/2}$ curve (D) of bare GCE, LDH-NO₃/GCE, LDH-SDS/GCE and LDH-DAB-CO-IL/GCE in 2.5 mM Fe(CN)$_6^{3-/4-}$ (1:1) solution containing 0.5 M KCl.

IL and the ability to adsorb both organic and inorganic compounds using electrostatic, dipole-dipole, ion-dipole and hydrophobic interactions correlation can result in enhanced electrochemical reaction rates and provide higher charge transfer compared with pure LDH or bare GC.

In order to investigate the features of surface modified electrodes, electrochemical impedance spectroscopy was performed in the frequency range of 0.1 to 10⁵ Hz with AC voltage amplitude of 0.18V. The Nyquist plots of bare GCE, LDH-NO₃/GCE, LDH-SDS/GCE, and LDH-DABCO-IL/GCE in 2.5mM [Fe (CN)$_6$]$^{3-/4-}$ containing 0.5M KCl were obtained and the results are shown in Fig. 1B. The charge transfer resistance ($R_{ct}$) of different electrodes were calculated from the semicircle portion of the Nyquist diagram. R$_{ct}$ values for bare GCE, LDH-NO₃/ GCE, LDH-SDS/GCE, and LDH-DABCO-IL/GCE are obtained as 1682, 1907, 4414 and 81, respectively. This demonstrated that the deposition of LDH-NO₃, LDH-SDS significantly decreased the conductivity of the electrode. In contrast, LDH-DABCO-IL/GCE accelerated the transfer of electron between the electrode and solution. In addition, the linear portion of the Nyquist plot in low frequency for LDH-DABCO-IL/GCE showed a controlled diffusion process on the surface of the electrode. The results were obviously in agreement with the CVs results, which confirm that the LDH-DABCO-IL has high electrical conductivity, high surface area, and excellent electrocatalytic activity. Hence, it was chosen as a modifier for future investigations.

*Electrochemical effective surface area*

The electrochemical effective surface area for bare GCE and LDH-DABCO-IL/GCE was calculated by the chronocoulometry method based on Eq. (1) given by Anson [16]:

$$Q(t) = \frac{2nFAcD^{1/2}t^{1/2}}{\pi^{1/2}} + Q_{dl} + Q_{ads} \qquad (1)$$

Where A is the surface area of the working electrode; c and D are the concentration and the diffusion coefficient of substrate, respectively (c= 2.5 mM of K₃[Fe(CN)$_6$, D=7.6×10$^{-6}$ cm² s$^{-1}$); $Q_{dl}$ is the charge of the double layer (that was corrected by background subtraction), and $Q_{ads}$ is the Faradic charge. The plots of $Q$–t and $Q$–t$^{1/2}$ are shown in Fig. 1C and 1D, respectively. Based on the slope of the linear relationship between $Q$ and t$^{1/2}$, A can be calculated to be 0.069 cm² and 0.19 cm² for GCE and LDH-DABCO-IL/GCE, respectively. The
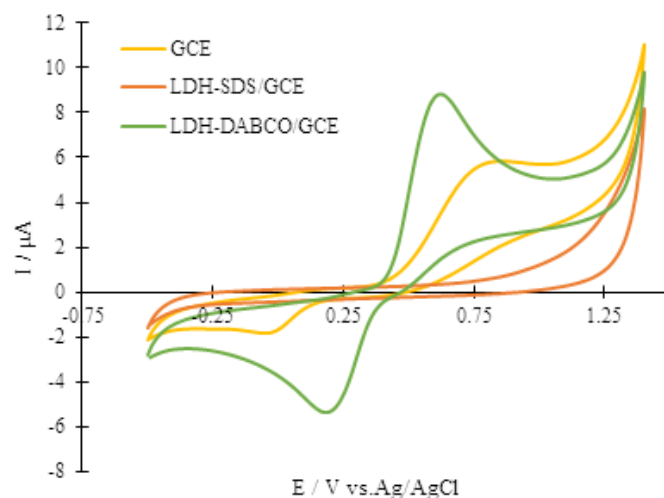
12

*Nanochem. Res., 9(1): 9-18, Winter 2024*

Fig. 2. CVs of 100 μM m-dopa recorded at bare GCE, LDH-SDS/GCE and LDH-DABCO-IL in 0.1 M ammonia buffer (pH=2). Scan rate: 50 mV.s$^{-1}$.

results indicated that the electrode's effective surface area was increased obviously after modifying GCE with LDH-DABCO-IL. As a result, the sensitivity of the electrode increased.

*Cyclic voltammetric behaviors of methyldopa*

Fig. 2 illustrates cyclic voltammograms of GCE, LDH-SDS/GCE, and LDH-DABCO-IL/GCE in the presence of 50 μM m-dopa at 50 mV.s$^{-1}$ in pH =2; only a small oxidation peak of m-dopa was observed with a high positive oxidation potential (0.63 V) at bare glassy carbon electrode. However, a significant enhancement in anodic current was achieved accompanying a low oxidation potential (0.20V) at the LDH-DABCO-IL/GCE modified electrode, which suggests that LDH-DABCO-IL is an effective mediator in the electrocatalytic oxidation of m-dopa. In addition, corresponding reduction peak of m-dopa was observed at both electrodes in pH=2, in comparison with GCE. Epc in LDH-DABCO-IL/GCE extremely decreased, while ipc dramatically increased. This indicates that the oxidation reaction is totally (ΔEp= 0.43) reversible, which is in agreement with previous reports [17-19].

In addition, no redox peak was observed at LDH-SDS/GCE, and the oxidation peak potential obtained at LDH-DABCO-IL/GCE was lower than that reported in the literature (see Table.1). Decreasing the oxidation potential indicates a facilitation of electron transfer between the electrode and m-dopa. Therefore, a remarkable decrease in oxidation overpotential was achieved

in the present study with LDH-DABCO-IL/GCE.

*pH effect*

According to a stacking of positive layers trapping anionic species in the interlayer domains, the lamellar structure of LDH, is greatly appropriate for anion diffusion. LDH is also considered as one of the main types of inorganic ion exchangers. Electrostatic interactions between hydroxylated sheets with positive charges as well as the exchanging anions have great effects on exchange in LDH. Likewise, anions with a great charge density have excellent exchange properties. Miyata [17] gave a comparative list of ions selectivities for monovalent anions: OH$^-$ > F$^-$ > Cl$^-$ > Br$^-$ > NO3$^-$ > I$^-$ and divalent anions: CO$_3^{2-}$ > C$_{10}$H$_4$N$_2$O$_8$S$^{2-}$ > SO$_4^{2-}$. Yamaoka et al. [18] characterized an equivalent selectivity sequence for divalent oxoanions: HPO$_4^{2-}$, HAsO$_4^{2-}$>CrO$_4^{2-}$> SO$_4^{2-}$> MoO$_4^{2-}$. Furthermore, it seems that the divalent anions selectivities are higher than those of monovalent anions. Based on the mentioned works, chloride and nitrate containing LDHs seem to be good options as optimum precursors for exchange reactions. More selective anions including Fe(CN)$_6^{2-}$, Fe(CN)$_6^{3-}$, Mo(CN)$_8^4$ can easily replace such anions.

The effect of different supporting electrolyte such as citrate, carbonate, phosphate and ammonia on the oxidation peak current of m-dopa was investigated. Preliminary experiments indicated that in the presence of carbonate and phosphate anions the electrochemical properties of modified electrode decreased. This observation may depend

*Nanochem. Res., 9(1): 9-18, Winter 2024*

13

Table 1. Comparison of the efficiency of some methods used in detection of methyldopa

| Method | Type of electrode | Modifier | $E_{ox}$ (V) | LOD ($\mu mol\ L^{-1}$) | Linear range ($\mu mol\ L^{-1}$) | Ref. |
|---|---|---|---|---|---|---|
| DPV[1] | Glassy carbon | Al/Mg LDH /DABCO | 0.25 | 0.076 | 0.23 - 860 | This work |
| DPV | Glassy carbon | $NiFe_2O_4$-MWCNTs[4] | 0.21 | 0.08 | 0.5–900.0 | [8] |
| DPV | Glassy Carbon | $Fe_3O_4$@$SiO_2$/GO nanocomposite | 0.21 | 0.086 | 0.1 - 400 | [9] |
| ASV[2] | Glassy Carbon | CMWCNTs | 0.21 | 0.08 | 0.1 – 300 | [13] |
| SWV[3] | Carbon | $Cu(OH)_2$ nanoparticle | 0.3 | 0.51 | 2.0 - 600.3 | [10] |
| SWV | Carbon paste | MWCNTs and p-chloranil | 0.12 | 0.2 | 0.5–165.5 | [17] |
| SWV | Carbon paste | Cellulose acetate | 0.1 | 5.5 | 34.8–70.3 | [18] |
| SWV | Carbon paste | CNTs[5] and ferrocene | 0.35 | 0.08 | 0.1–500 | [11] |
| SWV | Carbon paste | MWCNTs and ionic liquid | 0.45 | 0.1 | 0.4–400.0 | [7] |
| DPV | Carbon paste | $TiO_2$ nanoparticles and (FM)* | 0.36 | 0.08 | 0.02–100 | [4] |
| DPV | FTO | Fluorine doped $SnO_2$ | 1.1 | 2.9 | 0.2 – 60.0 | [12] |

[1] Differential pulse voltammetry
[2] Anodic stripping voltammetry
[3] Squarewave voltammetry
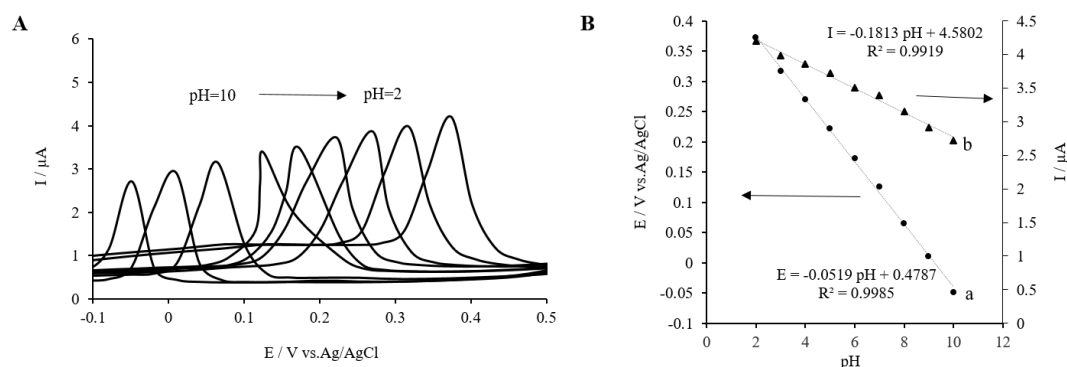[4] Multi-walled carbon nanotubes
[5] carbon nanotube



Fig.3. pH-dependence of peak potential(a) and peak current(b) related to the electro-oxidation of 100 µM m-dopa at LDH-DABCO-IL/GCE in 0.1 M ammonia solution.

on the substitution of chloride in the structure of DABCO-IL with phosphate or carbonate anions. Since in the presence of ammonia, electrochemical behaviors of modified electrode did not change, ammonia buffer was used in feature experiments.

The pH effect was investigated in the pH range of 2-10 using DPV technique in 0.1M ammonia buffer containing 50 µM m-dopa (Fig. 3A). The oxidation peak current of m-dopa was increased

by decreasing pH. The maximum current was observed in pH=2. According to the results, the oxidation peak potential shifted towards more negative potentials with increasing pH values, indicating that the methyldopa oxidation involves proton transfer. Additionally, the anodic peak potential shows pH dependence with a slope value of -51 mV.pH$^{-1}$ (Fig. 3B), commonly expected for the conversion of two-electron two-proton process
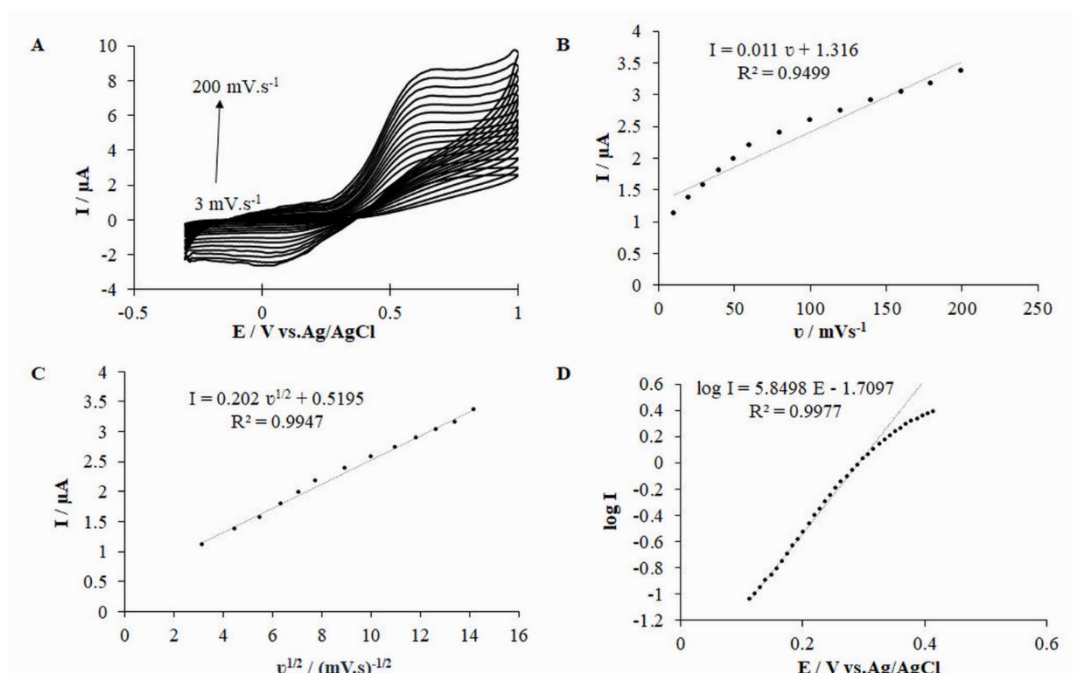
Fig.4. (A) CVs of LDH-DABCO-IL/GCE in presence of 0.5 mM m-dopa in 0.1 M ammonia solution (pH =2) at various scan rates: 5, 10, 25, 50, 75, 100, 150, and 200 mV.s⁻¹, respectively. Insets: (B) anodic peak current versus $v^{1/2}$ and (C) anodic peak current versus $v$ (D) logarithm of peak current versus anodic peak potential.

(Fig. S1) of m-dopa [19]. Consequently, ammonia buffer with pH 2.0 was selected as the supporting electrolyte in all voltammetric studies because of its higher peak current.

*Scan rate effect*

In order to study the nature of the electrode process, the effect of scan rate on oxidation peak current of m-dopa was recorded at different scan rates from 3 to 200 mV.s⁻¹ (Fig. 4A). As shown in Fig. 4C, the peak current increased linearly with the square root of the scan rate (correlation coefficient = 0.9947) which indicates that the oxidation reaction is influenced by the diffusion control process. For calculating the number of involved electrons in rate-determining step in oxidation of m-dopa, Tofel equation was used. The Tofel plot was drawn at a scan rate of 10 mV.s⁻¹ by using the rising part data of the anodic peak (Fig. 4D). According to the Tofel equation (Eq.2):

$$\log i = \log i_0 + \frac{(1-\alpha)nF}{2.303RT} E \qquad (2)$$

Where $\alpha$ is the electron transfer coefficient and n is the number of electrons transferred in the rate-determining step. The constants R, T and F represent their usual meanings, R=8.314 J K⁻¹mol⁻¹,

T=298 K, and F=96485 Cmol⁻¹. Using the slop of Tofel plot and by assuming n=1, the charge transfer coefficient of $\alpha$ = 0.65 was obtained.

*Interference*

In order to prove the feasibility of using sensor in real sample matrix, the effect of some interferences was studied. Hence, other species, which may exist in real samples matrix, were chosen as interfering agents and examined. As shown in Table 2, in the presence of 50.0 μM m-dopa, the concentrations of $Ca^{2+}$, $Mg^{2+}$, $Na^+$, $Ba^{2+}$, $SO_4^{3-}$, $Cl^-$, $NO_3^-$, ascorbic acid, oxalate, urea, glucose, sucrose, dopamine, levodopa, and uric acid did not significantly influence the height of the oxidation peak currents. The tolerance limit for the determination of m-dopa was set at concentrations where the error is less than 5.0%.

*Figure of merit of methods*

The determination of m-dopa concentration via LDH-DABCO-IL/GCE was conducted with DPV under optimized experimental conditions (Fig. 5A). According to the results, through two intervals of 0.24–33 μM and 33–860 μM, the oxidation peak currents were proportional to the m-dopa concentrations (Fig. 5B). As can be

Table 2. The influence of some interfering substances on the determination of 50.0 µM of MD.

| Interfering substances | Tolerance (mol Substance/mol Methyldopa) |
|---|---|
| Ascorbic acid | 200 |
| Oxalate | 500 |
| Urea | 400 |
| $Ca^{2+}, Mg^{2+}, Na^+, Ba^{2+}$ | 1000 |
| $SO_4^{3-}, Cl^-, NO_3^-$ | 1000 |
| Glucose, sucrose | 800 |
| Uric acid | 100 |

Table 3. Standard deviation (n=3), Darou Pakhsh, Pharmaceutical Mfg. Co. (Tehran, Iran).

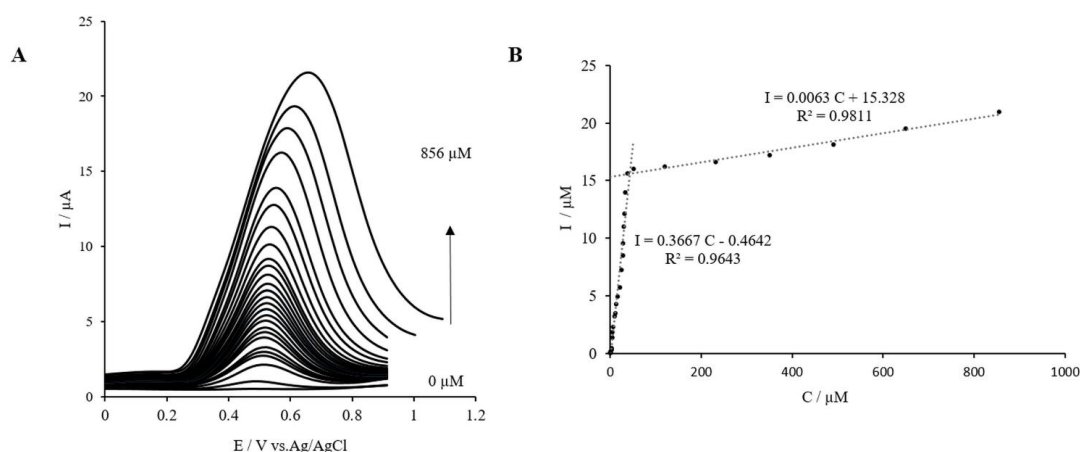| | Added (µM) | Expected (µM) | Found (µM) | Recovery (%) | RSD (%) |
|---|---|---|---|---|---|
| Tablet | - | 5.0 | 4.86± 0.1 | - | 0.44 |
| | 5.0 | 10.0 | 9.90±1.4 | 100.8 | 3.8 |
| | 10.0 | 15.0 | 14.61±0.79 | 97.5 | 0.99 |
| Urine | - | - | <LOD | - | - |
| | 5.0 | 5.0 | 5.01 | 100.2 | 1.95 |
| | 10.0 | 10.0 | 10.046 | 100.46 | 0.046 |



Fig.5. (A) Differential pulse voltammogram of m-dopa at DABCO/LDH/GCE in 0.1 M ammonia solution (pH=2) for successive additions of m-dopa (deposition potential: 0 mV, depositpn time: 60s) and (B) shows corresponding plot.

seen in Fig. 5, the linear regression equations for two regions are demonstrated in the diagrams. The detection limit for these measurements was calculated to be 0.076 µM (S/N = 3). In order to study the reproducibility (electrode-to-electrode) and repeatability (for one electrode), five electrodes were constructed under the same conditions and also five repeated experiments were performed via each electrode. The values of 1.99% and 1.75% RSD were obtained for reproducibility and repeatability of the fabricated electrodes along with the determination of the electrodes peak currents in solutions containing 50 µM of m-dopa.

*Quantification of methyldopa in pharmaceutical and urine samples*

Differential pulse voltammetric (DPV) determination of methyldopa in tablets was performed based on the regression equation. Table 3 shows the tablets analysis via the suggested process. The fabricated electrode obtained an average recovery value of 99.7% with an RSD% of 1.45%. The claimed value confirmed the results

16

*Nanochem. Res., 9(1): 9-18, Winter 2024*

of the drug analysis acquired from the suggested approach. The results of the suggested approach were also in close agreement with the standard USP approach with an average recovery value of 101.7%. Nevertheless, according to the obtained results of the suggested approach, the adopted approach can be employed for the determination of methyldopa in drug and urine samples.

## CONCLUSIONS

The methyldopa oxidation demonstrated a quasi-reversible response on a bare electrode. According to the obtained results, the voltammetric response of methyldopa was modified at LDH-DABCO-IL/GCE. Furthermore, there has been a reduction in the separation of the anodic and cathodic peak potentials for the redox couple of methyldopa. By using LDH-DABCO-IL as a modifier on the electrode surface, the voltammetric behavior of methyldopa was found to be more reversible. According to the results, the peak currents were proportional to the concentrations of methyldopa over two intervals in the range of 0.24–33 μM and 33–860 μM with a detection limit of 0.076 μM. The results demonstrated that the suggested approach modified peak separation from interfering compounds including AA and UA. Moreover, the potential for oxidizing methyldopa and the detection limit were reduced by this method. The obtained results verified the accuracy of the proposed approach which makes it applicable for the determination of methyldopa in pharmaceuticals and urine samples.

## CONFLICT OF INTEREST

The authors declare no conflicts of interest.

## REFERENCES

1. Keech C, Albert G, Cho I, Robertson A, Reed P, Neal S, et al. Phase 1-2 Trial of a SARS-CoV-2 Recombinant Spike Protein Nanoparticle Vaccine. New England Journal of Medicine. 2020;383(24):2320-32. https://doi.org/10.1056/NEJMoa2026920
2. Tortolini C, Di Fusco M, Frasconi M, Favero G, Mazzei F. Laccase-polyazetidine prepolymer-MWCNT integrated system: Biochemical properties and application to analytical determinations in real samples. Microchemical Journal. 2010;96(2):301-7. https://doi.org/10.1016/j.microc.2010.05.004
3. Shahrokhian S, Saberi R-S, Kamalzadeh Z. Sensitive Electrochemical Sensor for Determination of Methyldopa Based on Polypyrrole/Carbon Nanoparticle Composite Thin Film Made by In Situ Electropolymerization. Electroanalysis. 2011;23(9):2248-54. https://doi.org/10.1002/elan.201100169
4. Najafi K, Asadpour-Zeynali K, Mollarasouli F. Preparation of A Magnetic Nanosensor Based on Cobalt Ferrite Nanoparticles for The Electrochemical Determination of Methyldopa in The Presence of Uric Acid. Combinatorial Chemistry & High Throughput Screening. 2020;23(10):1023-31. https://doi.org/10.2174/1386207323666200521123657
5. Halakoei H, Ghalkhani M, Sobhani-Nasab A, Rahimi-Nasrabadi M. An efficient electrochemical sensor based on CeVO4-CuWO4 nanocomposite for methyldopa. Materials Research Express. 2021;8(8):085001. https://doi.org/10.1088/2053-1591/ac16f1
6. Fathi SA, Othman NS, Al-Taee AT. Indirect Spectrophotometric Method for Determination of Methyldopa in Pure and Pharmaceutical Formulation. Biomedicine and Chemical Sciences. 2023;2(2):149-54. https://doi.org/10.48112/bcs.v2i2.380
7. Gupta VK, Jain R, Radhapyari K, Jadon N, Agarwal S. Voltammetric techniques for the assay of pharmaceuticals--a review. Analytical biochemistry. 2011;408(2):179-96. https://doi.org/10.1016/j.ab.2010.09.027
8. Upadhyay K, Asthana A, Tamrakar RK. Extractive spectrophotometric determination of α-methyldopa in bulk dosage and in its formulations. Research on Chemical Intermediates. 2015;41(8):5521-8. https://doi.org/10.1007/s11164-014-1678-6
9. Shpigun LK, Ryabenko VS. Flow-injection method of spectrophotometric determination of catecholamines in pharmaceutical formulations. Theoretical Foundations of Chemical Engineering. 2012;46(4):419-23. https://doi.org/10.1134/S0040579512040070
10. Shaikh SMT, Manjunatha DH, Harikrishna K, Ramesh KC, Kumar RS, Seetharamappa J. Diazocoupling reaction for the spectrophotometric determination of physiologically active catecholamines in bulk and pharmaceutical preparations. Journal of Analytical Chemistry. 2008;63(7):637-42. https://doi.org/10.1134/S106193480807006X
11. Apetrei IM, Apetrei C. Study of Different Carbonaceous Materials as Modifiers of Screen-Printed Electrodes for Detection of Catecholamines. IEEE Sensors Journal. 2015;15(6):3094-101. https://doi.org/10.1109/JSEN.2014.2335534
12. Chitravathi S, Munichandraiah N. Simultaneous Determination of Catecholamines in Presence of Uric Acid and Ascorbic Acid at a Highly Sensitive Electrochemically Activated Carbon Paste Electrode. Journal of The Electrochemical Society. 2015;162(7):B163. https://doi.org/10.1149/2.0661507jes
13. Abolghasemi MM, Yousefi V, Piryaei M. Double-charged ionic liquid-functionalized layered double hydroxide nanomaterial as a new fiber coating for solid-phase microextraction of phenols. Microchimica Acta. 2015;182(13):2155-64. https://doi.org/10.1007/s00604-015-1553-1
14. Arenas LT, Gay DSF, Moro CC, Dias SLP, Azambuja DS, Costa TMH, et al. Brilliant yellow dye immobilized on silica and silica/titania based hybrid xerogels containing bridged positively charged 1,4-diazoniabicyclo[2.2.2] octane: Preparation, characterization and electrochemical properties study. Microporous and Mesoporous Materials. 2008;112(1):273-83. https://doi.org/10.1016/j.micromeso.2007.09.043
15. Fountoukis C, Nenes A. ISORROPIA II: a computationally efficient thermodynamic equilibrium model for K+-Ca2+-Mg2+-NH4+-Na+-SO42−-NO3−-Cl−-H2O

*Nanochem. Res., 9(1): 9-18, Winter 2024*

17

aerosols. Atmos Chem Phys. 2007;7(17):4639-59. https://doi.org/10.5194/acp-7-4639-2007

16. Cui L, Wu J, Ju H. Nitrogen-Doped Porous Carbon Derived from Metal-Organic Gel for Electrochemical Analysis of Heavy-Metal Ion. ACS Applied Materials & Interfaces. 2014;6(18):16210-6. https://doi.org/10.1021/am504367t

17. Ensafi AA, Saeid B, Rezaei B, Allafchian AR. Differential pulse voltammetric determination of methyldopa using MWCNTs modified glassy carbon decorated with NiFe2O4 nanoparticles. Ionics. 2015;21(5):1435-44. https://doi.org/10.1007/s11581-014-1291-0

18. Movlaee K, Ganjali MR, Aghazadeh M, Beitollahi H, Hosseini M, Shahabi S, et al. Graphene Nanocomposite Modified Glassy Carbon Electrode: As a Sensing Platform for Simultaneous Determination of Methyldopa and Uric Acid. International Journal of Electrochemical Science. 2017;12(1):305-15. https://doi.org/10.20964/2017.01.41

19. Ghoreishi SM, Saeidinejad F, Behpour M, Masoum S. Application of multivariate optimization to electrochemical determination of methyldopa drug in the presence of diclofenac at a nanostructured electrochemical sensor. Sensors and Actuators B: Chemical. 2015;221:576-85. https://doi.org/10.1016/j.snb.2015.06.129

20. Kang G-H, Park I-K. Reconstruction and intercalating anion exchange of ZnAl-layered double hydroxide. Ceramics International. 2022;48(3):3030-6. https://doi.org/10.1016/j.ceramint.2021.10.078

21. Zhang J, Wu S, Liu Y, Li B. Hydrogenation of glucose over reduced Ni/Cu/Al hydrotalcite precursors. Catalysis Communications. 2013;35:23-6. https://doi.org/10.1016/j.catcom.2013.01.017

22. Wang Z, Guo H, Gui R, Jin H, Xia J, Zhang F. Simultaneous and selective measurement of dopamine and uric acid using glassy carbon electrodes modified with a complex of gold nanoparticles and multiwall carbon nanotubes. Sensors and Actuators B: Chemical. 2018;255:2069-77. https://doi.org/10.1016/j.snb.2017.09.010

18

*Nanochem. Res., 9(1): 9-18, Winter 2024*